

The Detector DCR

Akiya Miyamoto *

High Energy Accelerator Research Organization (KEK),
1-1 Oho, Tsukuba, Ibaraki 305-0801, Japan

The Detector Concept Report(DCR) consists of two parts, one for the physics and the other for ILC detectors. It has been prepared as the accompany document of the ILC Reference Design Report. The overview of the detector part of the DCR and the plan for the final release is presented in this talk.

1 Introduction

The preparation of the DCR has been started since LCWS2006 at Bangalore[1]. Four editors for the detector part, Ties Behnke, Chris Damerell, John Jaros and Akiya Miyamoto, have worked together with authors of sub-sections to prepare the document. The preliminary version has been open to the community after the workshop at Beijing (BILCW07)[2]. Taking into account comments from the community as well as those from the Review Panel, it is scheduled to be released in August this year[4].

The goal of the Detector DCR is to make the case that detectors can do the ILC physics, showing detector designs are within our reach, where we are in detector developments and where we are going. On the other hand, the DCR is neither a complete description of a detector nor a review of the ILC detector concepts. The detector DCR is based on Detector Outline Documents (DODs)[6, 7, 8, 9] prepared by four detector concept teams last year as well as new studies since then, but a little focus is put on concept specific issues.

Selected topics of the detector DCR is presented in the next section and the plan for the final release is described in the subsequent section.

2 Overview of the Detector DCR

The goal of the ILC physics includes understanding of the mechanism of mass generation and electroweak symmetry breaking, searching for and perhaps discovering supersymmetric particles and confirming the principle of supersymmetry, and hunting for signs of extra space-time dimensions and quantum gravity[5]. The ILC detectors have to be optimized for these ILC physics targets.

Experimental conditions at the ILC provide an ideal environment for the precision study of elementary particle interactions, thanks to the clean signal conditions and well-defined initial state. Events are recorded without a bias which might be caused by an event trigger. However, the physics poses challenges on detector performances, pushing the limits of jet energy resolution, tracker momentum resolution, and vertex impact parameter resolution, as well as full solid angle coverage. Although benign by LHC standards, the ILC environment poses some interesting challenges of its own.

The world-wide linear collider physics and detector community has worked on these challenges and made impressive progresses. Four teams, GLD[6], LDC[7], SiD[8] and 4th[9], have formed to study detector concepts for the ILC experiments. They have reported their

*Representing co-editors: Ties Behnke, Chris Damerell and John Jaros

studies as the Detector Outline Documents (DODs) last year, and have kept continuing concept studies. GLD, LDC, and SiD are equipped with a granular calorimeter for particle flow measurements, while 4th aims to achieve a good jet energy resolution by a dual-readout calorimeter. Key parameters of the four detector concepts are summarized in Table 1.

Table 1: *Some key parameters of the four detector concepts. See Table 3 for magnet parameters.*

	GLD	LDC	SiD	4th
VTX	pixel	pixel	pixel	pixel
R_{in}/R_{out} (cm)	2.0/5.0	1.6/6.0	1.4/6.1	1.5/6.1
Main Tracker	TPC[Si]	TPC[Si]	Si	TPC(drift)
R_{in}/R_{out} (TPC[Si]) (cm)	45/200[9/30]	30/158[16/27]	20/127	20/140
L_{half} (TPC[Si]) (cm)	230[62]	208[140]	168	150
# barrel points (TPC[Si])	200[4]	200[2]	5	200(120)
ECAL	Scinti.-W	Si-W	Si-W	Crystal
Barrel R_{in}/L_{half} (cm)	210/280	160/230	127/180	150/240
# X_0	27	23	29	27
HCAL	Scinti.-Fe	Scinti.-Fe	RPC/GEM-W	fiber Dream
Barrel R_{in}/L_{half} (cm)	229.8/280	180/230	141/277.2	180/280
Interaction length	5.8	4.6	4.0	9
Overall Detector				
R_{out}/L_{half} (cm)	720/750	600/620	645/589	550/650

In parallel to the concept studies, R&D on detector technologies have been pursued actively world-wide[10]. Inter-concept teams have been formed to address R&D issues common to concepts.

The detector DCR is based on these activities, but with a little emphasis on concept specific issues.

2.1 Challenges for Detector Design and Technologies

The relatively low radiation environment of the ILC allows detector designs and technologies not possible at the LHC, but the demanding physics goals still challenge the state of the art technologies.

Many of the interesting physics processes at the ILC appear in multi-jet final states, often accompanied by charged leptons or missing energy. The reconstruction of the invariant mass of two or more jets will provide an essential tool for identifying and distinguishing W 's, Z 's, H 's, top and discovering new particles. To distinguish W 's and Z 's in their hadronic decay mode, the di-jet mass resolution should be comparable to their natural width, say a few GeV or less. The jet energy resolution of $\sigma_E/E < 3 \sim 4\%$ ($30\%/\sqrt{E}$ for jet energies below about 100 GeV), which is about a factor of two better than that achieved at LEP, will provide such di-jet mass resolution. A factor of two improvement in jet energy measurement improves the resolution of the Higgs mass measurement using the four-jet mode of the Higgsstrahlung process by about 20% as shown in Figure 1. It is equivalent to a luminosity gain of about 40%. A similar gain of performance is expected in measurements of such as $\Delta\text{Br}(H \rightarrow WW^*)$ and the Higgs self-coupling.

The Higgs measurement from di-lepton recoil mass is important because it is measured without any assumption on its decay mode. In order to measure the Higgs mass at a precision close to the ultimate limit set by the initial beam energy spread, the momentum resolution of the tracking system ($\Delta p_t/p_t$) has to be less than $1 \times 10^{-3} \oplus 5 \times 10^{-5} p_t$ (GeV/c). Such a high-performance tracking device allows measurements of the center of mass energy

at about 20 MeV precision by using the process, $e^+e^- \rightarrow \mu^+\mu^-(\gamma)$. In the measurement of the slepton mass using the end point of lepton momentum, a gain of about 40% in luminosity is expected if the momentum resolution improves from from $8 \times 10^{-5} p_t$ to $2 \times 10^{-5} p_t$.

Efficient and clean identification of bottom and charm quark jets are indispensable methods to carry out the ILC physics program. For example, the identification of b and c jets in Higgs decays are essential to measure Yukawa couplings of c and b quarks. b jets identification in the top quark decays are useful to reduce combinatorial background in finding a correct jet combination of their hadronic decay. Quark charge measurements of jets through an efficient reconstruction of secondary and thirdly vertices would be a key method for studies of forward-backward asymmetries of b quark. The vertex detector which could measure the impact parameter at precision better than $5 \oplus 10/p \sin^{3/2} \theta$ (μm) will provide the performance to carry out these physics.

Sub-detector performances needed for key ILC physics measurements are summarized in Table 2.

Table 2: Sub-Detector Performance Needed for Key ILC Physics Measurements.

Physics Process	Measured Quantity	Critical System	Critical Detector Characteristic	Required Performance
ZHH $HZ \rightarrow q\bar{q}b\bar{b}$ $ZH \rightarrow ZWW^*$ $\nu\bar{\nu}W^+W^-$	Triple Higgs Coupling Higgs Mass $B(H \rightarrow WW^*)$ $\sigma(e^+e^- \rightarrow \nu\bar{\nu}W^+W^-)$	Tracker and Calorimeter	Jet Energy Resolution, $\Delta E/E$	$3 \sim 4 \%$
$ZH \rightarrow \ell^+\ell^-X$ $\mu^+\mu^-(\gamma)$ $HX \rightarrow \mu^+\mu^-X$	Higgs Recoil Mass Luminosity Weighted E_{cm} $B(H \rightarrow \mu^+\mu^-)$	Tracker	Charged Particle Momentum Resolution, $\Delta p_t/p_t^2$	5×10^{-5}
$HZ, H \rightarrow b\bar{b}, c\bar{c}, gg$ $b\bar{b}$	Higgs Branching Fractions b quark charge asymmetry	Vertex Detector	Impact Parameter, δ_b	$5\mu\text{m} \oplus 10\mu\text{m}/p(\text{GeV}/c) \sin^{3/2} \theta$

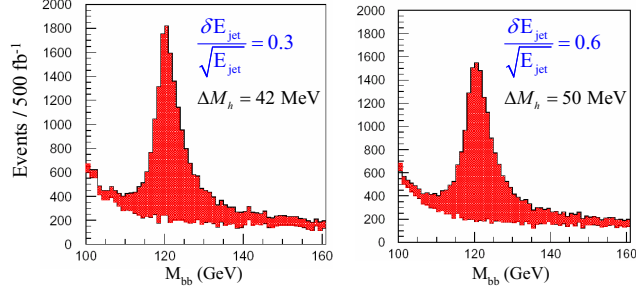


Figure 1: Reconstructed Higgs di-jet invariant mass for different jet energy resolutions. The analysis has been performed for a center of mass energy of 350 GeV and a total integrated luminosity of 500 fb^{-1}

2.2 Machine Detector Interface

The ILC beam induces following backgrounds; disrupted beam, photons and low energy electron-positron pairs generated by beamstrahlung; synchrotron radiation created when beam pass through beam line magnets; muons created by interactions between beam halo and collimators; neutrons created by electron-positron pairs and disrupted beam hitting beam line components; hadrons and muons created by photon-photon interactions.

A careful design of shields against these backgrounds is crucial. Their impacts on detector performances have been studied based on Monte Carlo simulations and estimated background hit rates have been below critical level so far. For an example, a hit occupancy in TPC due to the electron-positron pair background has been estimated by a simulation. TPC takes 100 bunch crossing(BX) of time to readout an event. After superimposing 100 BX of background hits, the hit occupancy is less than 0.2%, which is well below the critical occupancy of 1%.

Concerning the detector integration, the baseline plan is to assemble most of the detectors on surface, then brought them down the underground experimental hall for final assembly. This is to minimize the size of the underground experimental hall and to save the detector construction time.

The baseline design of the ILC foresees one interaction region, equipped with two detectors. The two detectors are laid out in such a way that each can be moved quickly in and out the interaction region thus allowing the sharing of luminosity between both detectors (push-pull operation). Details such as switchover time and frequency are still under discussion and a system with two beam delivery lines will be kept as an option until the detailed engineering design study demonstrates the feasibility of such a push-pull scheme.

2.3 Subsystem Design and Technologies

Technologically oriented description of detector sub-systems for a ILC detector is described in this section, aiming to show what kind of technologies exists for them, their challenges, and required R&Ds to achieve goals.

2.3.1 Vertex Detector

Four to six layers of silicon pixel detectors are used for a vertex detector. In total there are about $10^9 \sim 10^{10}$ pixels of size of about $20 \mu\text{m}^2$ or less. The beam pipe radius is 15 mm or less to place the vertex detector as close as to the interaction point. The thickness of each layer of the vertex detector is 0.1% X_0 or less. The vertex detector has to be reasonably hard against radiation and beam induced RF radiation (EMI). To keep background hits occupancy low, it has to be readout our fast or store locally and readout between the beam pulse. Due to a unique feature of the ILC beam structure, which has about 200 msec of quiet period after 1 msec of beam collisions, data of all collisions have to be read out without a front-end trigger for software filtering at later stages. To reach the performance goal, a calibration of internal alignment has to be carefully designed and an effect of powering and cooling to detector alignments should be minimum. There are no proven vertex detector technology to meet the performance goal under the ILC operational condition and R&Ds on more than 10 technologies are pursued worldwide extensively.

2.3.2 Silicon Strip Tracker

Silicon strip tracker is used as the main tracker of SiD concept and intermediate, forward or endcap trackers of other concepts. The silicon strip tracker is robust against unexpected radiation backgrounds; it is fast such that signal charges are collected before the next bunch crossing and an impact of beam backgrounds are minimum; it is precise such that point resolutions of $5 \sim 10\mu\text{m}$ are achievable. While silicon strip detector has been used extensively in other experiments, large detector system has typically $2\%X_0$ of material per layer. The most of them is attributable to dead material needed for support, cooling and readout. This dead material is a source of a performance deterioration. To significantly reduce these dead material while keeping the benefits of silicon strip detectors is one of the most significant challenges of R&Ds for silicon tracking at the ILC[4].

2.3.3 Gaseous Tracker

Time Projection Chamber (TPC) is considered as a main tracker by GLD, LDC and 4th concepts. The tracking of the TPC is robust because of many three-dimensional point measurements along the track. Material in the tracking volume is minimum and particle identification is possible. Detectors such as GEM[11] and MicroMegas[12] are candidates for the endplate detector, in order to meet the goal of the momentum resolution, Beam tests of a small test system suggest that the performance goal is within the technology in hand. Still a design to minimize a positive ion build up in the drift volume has to be developed and a gas with lowest diffusion and less contamination of Hydrogen atoms should be investigated. Operatability in non-uniform magnetic field caused by the anti-DID magnet and design of end-plate electronics with short radiation length is another challenge of the TPC R&D. International collaboration, LCTPC[13], is formed and pursuing these studies.

2.3.4 Calorimeter

Calorimeter is a key device to achieve a good jet energy resolution. The GLD, LDC and SiD concepts are equipped with a particle flow calorimeter, which is characterized by a highly granular segmentation both in lateral and longitudinal directions. A sandwich structure of absorbers and small sensors are adopted. Both electromagnetic and hadron calorimeters are placed in side the coil of the detector solenoid magnet. In the particle flow analysis, charged particle signals in the calorimeter are set aside by using tracker information, and calorimeter information is used only to measure neutral particle energies. Therefore, the high granularity in calorimeter segmentation and an excellent shower reconstruction algorithm are crucial. On the other hand, 4th concept is equipped with a dual read out calorimeter: scintillating fibers for all charged particles in a shower and clear fibers for Cherenkov light induced by electrons and positrons. Despite its few longitudinal sampling, it aims at a good jet energy resolution with a high resolution calorimeter.

A development of calorimeter technologies is one of the most active area of the ILC detector R&D[4] and many technologies are currently pursued, for example; for electromagnetic calorimeter, sandwiches of tungsten or lead absorber and silicon, MAPS, or scintillator and semiconductor photon sensor readout; for hadron calorimeter, lead or iron as absorber and scintillator and photon sensor readout, gas chamber and GEM or RPC readout.

Table 3: Summary of the parameters of ILC detector magnet, compared with that of CMS.

	unit	CMS	GLD	LDC	SiD	4th(In/Out)
Magnetic Field	Tesla	4	3	4	5	3.5/1.5
Coil Radius	m	3.25	4	3.16	2.65	3/4.5
Coil Half length	m	6.25	4.43	3.3	2.5	4/5.5
Stored Energy(E)	GJ	2.6	1.6	1.7	1.4	5.7
Cold mass (M)	ton	220	78	130	117	
E/M	kJ/kg	12.3	20	13	12	

2.3.5 Superconducting Magnet

A detector magnet is one of the major part of the detector cost. The GLD, LDC and SiD concepts use a large bore coil, while 4th concept use a dual coil system where the outer coil is used instead of iron flux return. Typical parameters of them are summarized in Table 3. As seen in the table, the parameters of the magnet for the ILC detector is similar to the CMS magnet and it's experience is useful.

2.3.6 Data Acquisition

The ILC RF system is operated at the frequency of 5Hz. During the beam period of 1 msec, the collision rate is about 3 MHz. A pipeline system is mandatory to record data of all collisions. The burst collision is followed by about 200 msec of a quiet time. Thus average event rate is about 15kHz, which is moderate compare to LHC. No hardware trigger is planned and event selection is done by software after readout data of all bunch collisions. On the other hand, zero suppression and data compression at detector front ends are important to minimize a load to the data acquisition system, because the ILC detectors are equipped with high granularity sensors.

2.3.7 Luminosity, Energy, and Polarization

The beam energy should be know to be less than 100 ppm precision for the precise Higgs recoil mass measurement. For physics at GigaZ or W threshold, it is required to be less than 50 ppm. About 200 ppm has been achieved at LEP and SLC. Several R&Ds[4] are in progress to achieve a factor of 2 or more improvement. These R&Ds include the studies on developments of a high precision beam position monitor to measure beam energy using upstream beam line magnets as a spectrometer; the beam energy measurement by detecting synchrotron lights emitted from downstream beam line bending magnets; and the measurement of the energy weighted luminosity from lepton's acollinearity of processes such as Bhabha and $\mu\bar{\mu}(\gamma)$.

Beam polarization should be measured at precision better than 0.5%. A gain in physics potential is anticipated if $\Delta P \sim 0.25\%$ or less. It is measured by Compton polarimeters at upstream and down stream of IP. Developments of the instruments for the Compton measurements is important.

2.3.8 Test beams

Detector R&D requires supports by test beam resources. Resources are limited and optimal coordination world wide is necessary. Test Beams working group has been organized by WWS and the first report has been presented[14].

2.4 Sub detector performance

Each concept team has developed their own detector full simulator and reconstruction tools and pursued studies on performances of such as vertexing, tracking, jet reconstruction and so on. It is impossible to cover all results here and only typical ones are shown. Performances are more or less similar among the concepts.

The tracking performance has been studied for both TPC and Silicon main tracker. For the TPC main tracker, the track finding efficiency has been studied using Z pole events where Z decays to $d\bar{d}$. The obtained the efficiency exceeded 99%, though realistic effects such as those by a non-uniform magnetic field, space charges and background hits have yet to be taken into account. SiD adopts an inside-out tracking finding method, where the vertex detector is used to find a seed track. According to this method, the efficiency of about 99% is achieved for a track whose origin is within 1 cm from the IP using a sample of $e^+e^- \rightarrow Z \rightarrow q\bar{q}$ events at 500 GeV center-of-mass energy. The momentum resolution of the tracking device has been studied by the GLD. Combining information of TPC, the intermediate tracker and the vertex detector, the momentum resolution is found to be consistent with the goal of $\Delta p_t/p_t \sim 10^{-3} \oplus 5 \times 10^{-5} p_t$ (GeV/c).

Impact parameter resolutions of the tracking system have also studied by each concept teams and found to be consistent with the performance goal.

As already pointed out in the subsection 2.1, the pure and efficient tagging of b quark and c quark jets is important for the ILC physics. The topological vertexing as pioneered by SLD has the potential for such a high performance tagging. The code has been ported for studies of ILC detectors. An initial result of its study is shown in Figure 2[15]. The obtained purity and efficiency using a realistic detector model is promising.

GLD, LDC and SiD all utilize sampling calorimeters, whose energy resolution is essentially determined by the sampling fraction. For single particles, the energy resolution of the electromagnetic calorimeters ranges from 14 to $17\%/\sqrt{E}$ for the stochastic term and those for the hadron calorimeter ranges from 50 to $60\%/\sqrt{E}$. For jet energy measurements, the particle flow analysis (PFA) is crucial to achieve the required level of performance. At the ILC detectors, the trackers can measure charged particles better than the calorimeters.

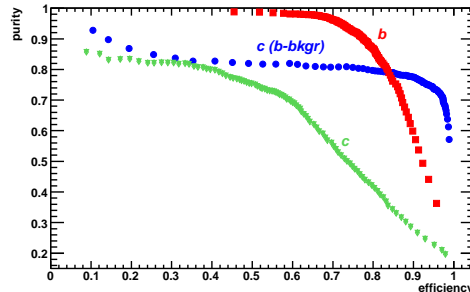


Figure 2: Efficiency and purity for tagging a b -quark (red square) and c -quark (green triangle) jets in Z decays, using a full simulation. The blue-circle points indicate the further improvement in performance of the charm tagging in events with only bottom background is relevant.

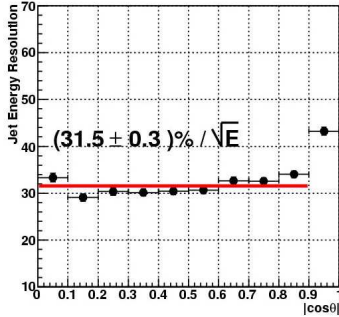


Figure 3: *The stochastic term of the jet energy resolution ($\sigma_{90}/\sqrt{E_{jet}}$) as a function of $|\cos\theta_{jet}|$ in the case of $e^+e^- \rightarrow q\bar{q}$ (light quarks only) events at Z pole energy. A result by GLD-PFA for the GLD detector.*

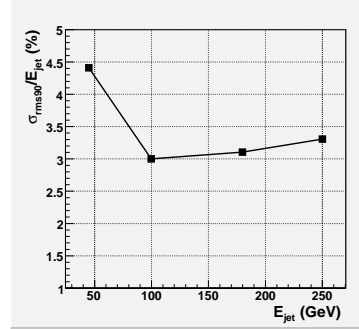


Figure 4: *The relative jet energy resolution, σ_{90}/E_{jet} , of PandoraPFA averaged in the region $|\cos\theta_{jet}| < 0.7$, as a function of the jet energy.*

Thus, in the PFA, tracker signals are used to get charged particle information and calorimeter signals are used only to reconstruct neutral particles. Since calorimeter is sensitive to charged particles as well, it is essential to develop a sophisticated algorithm to fully utilize the fine granularity of the calorimeters, identify and remove the calorimeter signals produced by charged particles.

To this end, PFA algorithm have been studied extensively by many groups. For an example, the algorithm such as WolfPFA[16] and GLD-PFA[17] consists of following steps; cluster calorimeter signal cells; discard clusters whose position and energy are matched with extrapolated charged tracks and use tracker information for such particles; consider remaining clusters as neutral particles and use calorimeter information. The PandoraPFA[18] uses the similar approach but introduced algorithm of re-clustering to disconnect merged clusters or reconnect divided clusters, resulting better performance. Another approach includes the algorithm to use the charged track information as a seed of the calorimeter clustering[19].

The performance of the GLD-PFA has been studied using the Z pole events where Z decays to u , d or s quarks only. The distribution of the observed particle energy tends to have two-gaussian distribution, broader one being caused by a loss of particles due to imperfect acceptance. σ_{90} is introduced as a measure of the PFA performance. σ_{90} is defined as the RMS of samples containing 90% of all samples. The resultant performance is shown in Figure 3 as a function of the jet angle.



Figure 5: *Jet energy resolution in terms of σ_{90}/\sqrt{E} obtained with PandoraPFA and the Tesla TDR detector model plotted as a function of TPC outer radius and magnetic field.*

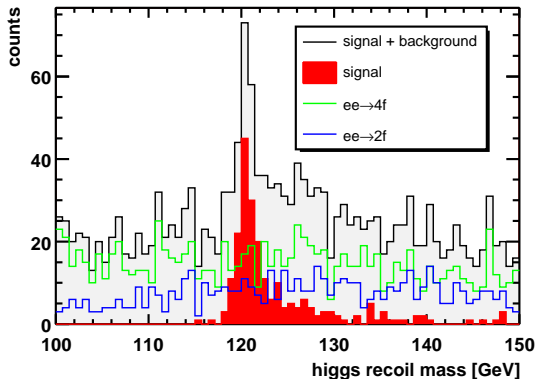


Figure 6: Recoil mass spectrum reconstructed for a 120 GeV Higgs, with full background simulation.

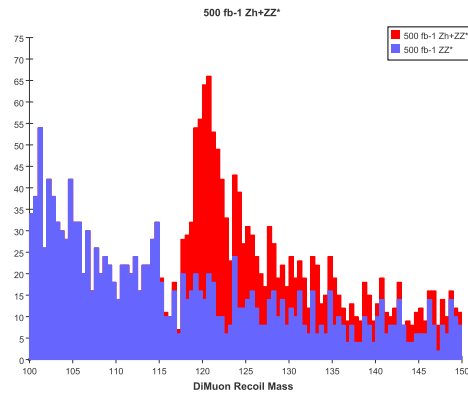


Figure 7: Di-muon recoil mass for ZZ^* background (blue) and ZH signal plus background (red) for centrally produced muons.

In the central region of $|\cos\theta_{jet}| < 0.9$, the obtained resolution is consistent with the goal.

However, for higher energy jets, the resolution of GLD-PFA gets worse and not satisfactory. On the otherhand, the PandoraPFA has successfully updated its algorithm recently and the resolution of about $30\%\sqrt{E}$ has been achieved for a jet of energy up to 100 GeV. The jet energy dependence of the energy resolution ($\Delta E/E$) of Pandora PFA is shown in Figure 4. Further improvements of the performance are anticipated because studies using a perfect PFA indicates that improvements in the resolution for high energy jets would be achievable.

The number of detector optimization studies have been performed with the PandoraPFA. For example, Figure 5 shows how the jet energy resolution depends on TPC radius (which is almost the same as the inner radius of calorimeter) and magnetic field. This study is suggesting that the resolution improves with increasing the magnetic field strength but the larger radius of the calorimeter is more important than the stronger magnetic field.

The dual readout calorimeter system of the 4th concept does not have longitudinal segmentation, thus the jet energy is determined mainly by the calorimeter after the jet clustering using the cone algorithm. The tracker information is used to correct low p_t tracks. The energy resolution of about $40\%\sqrt{E}$ has been reported[20].

2.5 Integrated Physics Performance

In this paper, studies on the Higgs recoil mass measurement and on the $\nu\bar{\nu}b\bar{b}$ channel of the Higgsstrahlung process are presented. A few more physics studies are described in the DCR. The scope of the studies in this section is rather limited and does not cover the full physics potential of ILC. The purpose of this section is to illustrate the level of maturity of both the understanding of the detectors and of the reconstruction and analysis algorithms. Especially, development of the particle flow algorithms is still advancing rapidly. Therefore results presented in the following should be interpreted as a snapshot of an ongoing development, where significant further improvements can be expected in coming years.

The one of the most challenging reactions for the tracking system of the ILC detector is the measurement of the Higgs mass using the recoil mass technique. LDC has studied both $H\mu\mu$ and Hee final states of $e^+e^- \rightarrow ZH$ process near threshold ($\sqrt{s} \sim 250$ GeV), including background processes of 4 fermions and 2 fermions final states. Based on a data sample equivalent of 50 fb^{-1} , a signal from the Higgs has been reconstructed as shown in Figure 6. From a simple fit to the mass distribution, the error of Higgs mass measurement is estimated to about 70 MeV and the relative cross section error being 8%.

A similar analysis has been performed in the context of the SiD detector concept, at a center of mass energy of 350 GeV. The analysis fully simulated the machine background events as well. The background events have been combined with the signal events at the Monte Carlo hit level prior to digitization, then fed into a full track reconstruction code. Requiring two muons with momentum greater than 20 GeV, events whose invariant mass of the two-muon system is consistent with Z were selected. Figure 7 shows the recoil mass distribution for the ZZ^* background in blue and ZH signal plus background in red. The precision of the Higgs mass from this measurement, based on a comparison between the mass distribution reconstructed and template Monte Carlo distributions, is estimated to be 135 MeV. Taking in to account the larger center of mass energy of this analysis, the result is consistent with the previous analysis.

GLD has studied the process, $e^+e^- \rightarrow ZH$ at the center of mass energy of 350 GeV, where Z decays to invisibly and H decays to jets and the Higgs mass is $120 \text{ GeV}/c^2$. In this case, compared to the four-jet mode, a beam energy constraint does not work for improve measurements due to the missing particles. But there is no ambiguity in the mass measurement due to exchanges of colored particles in the final state because all of visible particles stem from the Higgs decay. Thus high-performance PFA measurements is crucial for a good measurement. $e^+e^- \rightarrow ZZ$ is the major background process and an excellent vertex detector is a key to reject them by discarding non- b quark jets.

The preliminary result of GLD is shown in Figure 8. The analysis was based on a Monte Carlo sample of 200 fb^{-1} . The effects of beamstrahlung as well as bremsstrahlung were included in the event generation. The Higgs signal is clearly seen above backgrounds, while further improvements of PFA performance is awaited to achieve the signal width consistent with $30\%\sqrt{E}$.

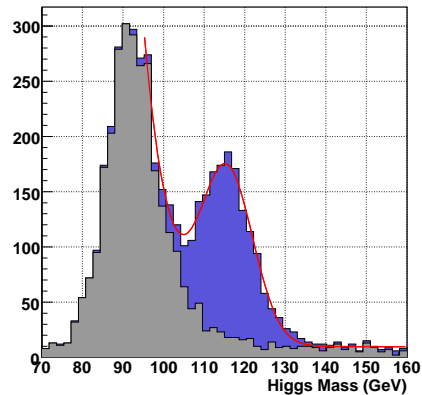


Figure 8: *Reconstructed mass spectrum for Higgs candidates in the $ZH \rightarrow \nu b \bar{b}$ decay.*

2.6 The case for two detectors

Two complementary detectors are crucial for ILC, because it offers competing experiments, cross checking of results and scientific redundancy for precision measurements at the level

which is not created by more than one analysis teams for one detector; significant increase of the scientific productivity, despite the splitting of the ILC luminosity; maximal participation of the global particle physics community; the backup if one detector needs significant down time. There are numerous historical examples where complementary experiments were critical. Further arguments will be found in Ref.[21].

2.7 Costs

The Costing Panel has been formed by WWS to estimate costs of each concept by a common approach. They have estimated the costs in light of the GDE costing rule and attempt to identify breakdown and cost drivers. The cost breakdowns are different among concepts depending on how to categorize items, for example, a separation or inclusion of M&S and man power costs. But, as naturally expected, calorimeters and magnets are the cost drivers. Overall, there is a reasonable agreement among estimates by GLD, LDC and SiD and the total cost lies in the range of 400 ~ 500 M\$ with about 20% error.

2.8 Options

The one option is GigaZ, which aims to run at Z pole energy with a luminosity of $\sim 4 \times 10^{33} \text{cm}^{-2}\text{s}^{-1}$ and accumulate 10^9 Z events in one year. Despite the high event rate, the event overlap probability is less than 1% and not a problem. Challenges are to run with a polarized positron beam with a frequent change of its polarity in order to reduce systematics and measure the beam energy at precision less than 3×10^{-5} .

The other is Photon Collider for experiments of $\gamma\gamma$ and $e\gamma$ collisions. It provides a novel opportunity of physics such as studies of $\Gamma(H \rightarrow \gamma\gamma)$ and CP properties of the Higgs. To make a $\gamma\gamma$ collision in the ILC, the beam lines have to be modified to change the crossing angle from 14 mrad to around 25 mrad. In addition, a $\gamma\gamma$ beam dump system has to be developed, to deal with the γ energy after collision: the γ beam is collimated and has the energy of about 50% of the initial beam, but can not be steered or smeared out by magnets like e^+/e^- beams. For Photon Collider experiments, near beam line components of detectors has to be modified to open a space to inject a laser light and to extract γ beams. Additional space in a detector hall may be necessary for a laser optical cavity.

3 Comments

Editors appreciate for your patient reading of the draft and sending us valuable comments. We have received many technical comments, which will be included in the next version to be released after the workshop. There are another class of comments, where inputs from community are crucial.

One is regarding the goal of the jet energy measurement. It has been set as $\Delta E/E \sim 30\%/\sqrt{E} \oplus \text{const.}$, where the constant terms are usually neglected. This goal is to achieve a jet-pair invariant mass resolution ($\Delta M_{12}/M_{12}$) which is sufficient to separate W and Z in their hadronic decay modes. The mass resolution of the jet pair is approximated, in terms of the jet energy resolution ($\Delta E_i/E_i; i = 1, 2$), as

$$\frac{\Delta M_{12}}{M_{12}} \sim \frac{1}{2} \left(\frac{\Delta E_1}{E_1} \oplus \frac{\Delta E_2}{E_2} \right), \quad (1)$$

where the mass of the jets and the error of the angle between the jets are neglected. For higher energy jets, the jet energy resolution is dominated by the constant term which would be mainly determined by a limitation of the PFA performance. Therefore, it would be more appropriate to express the goal of the jet energy resolution in terms of $\Delta E/E$ rather than the coefficient of the stochastic term. On the other hand, physics studies have been carried out assuming the formula, $\Delta E/E \sim \alpha/\sqrt{E}$ and studies assuming constant $\Delta E/E$ are yet to be done. The PFA performances will improve time to time and conservative opinions to keep the original arguments for the DCR have been made.

One another issue is regarding the momentum resolution: what do we gain by having the resolution which is significantly better than the original goal of $1 \times 10^{-3} \oplus 5 \times 10^{-5} p_t$? If the di-lepton recoil mass of the process, $e^+e^- \rightarrow ZH$, is measured at $\sqrt{s} = 350$ GeV for $M_h = 120$ GeV, the resolution improves with better momentum resolution. On the otherhand, as long as this measurement is concerned, much better performance is obtained if measured just above the threshold.

The statement in the draft DCR will be rephrased taking account these arguments.

4 Summary

The overview of the draft detector DCR is presented. The detector DCR describes detector designs, R&Ds on detector technologies, and expected performances, aiming to make the case for the ILC detectors.

The author of the DCR consists of those who have participated in the detector concept studies, linear collider detector R&D or have an interest in the physics and detectors for ILC. Those who are qualified are invited and encouraged to sign the DCR. The web page has been prepared for the sign up.

The draft is open to the public at <http://www.linearcollider.org/wiki> and comments from the community is welcomed. The DCR Review Panel has been formed by WWS. Preliminary comments from the panel is due by the end of LCWS2007 and the final report is expected by the beginning of July. Taking into accounts these comments, the DCR is scheduled to submit to ILCSC in August.

Acknowledgments

The author wish to thank co-editors of the detector DCR whose help is indispensable for this talk: Ties Behnke, Chris Damerell, John Jaros. Moreover, the author would like to appreciate many colleagues of the ILC community whose work has been reported in the detector DCR. This work is partially supported by the Creative Scientific Research Grant No. 18GS0202 of the Japan Society for Promotion of Science.

References

- [1] LCWS2006, <http://www.tifr.res.in/~lcws06/>.
- [2] Beijing Workshop, <http://bilcw07.ihep.ac.cn/>.
- [3] See, <http://www.linearcollider.org/cms/?pid=1000025>.
- [4] The Detector RDR is released as the detector volume of RDR this summer. It is now available at the RDR web site[3] together with other volumes on Executive Summary, Physics and Accelerator. Details on ILC detectors will be found in the detector volume of RDR.
- [5] For example, see P. Zervas, in these proceedings; the physics volume of RDR[3].

- [6] K. Abe *et al.*, *GLD Detector Outline Document*, arXiv:physics/0607154 (2006).
- [7] D. Kiseilewska *et al.*, *Detector Outline Document for the Large Detector Group*, <http://www.ilcldc.org/documents/dod/> (2006).
- [8] The SiD Concept Group, *SiD Detector Outline Document*, <http://hep.uchicago.edu/~oreglia/siddod.pdf> (2006).
- [9] Patric Le Du *et al.*, *Detector Outline Document for the Fourth Concept Detector at the International Linear Collider*, <http://www.4thconcept.org/4doc.pdf> (2006).
- [10] ILC Detector R&D Panel Website, <https://wiki.lepp.cornel.edu/ilc/bin/view/Public/WWS/>.
- [11] F. Sauli, Nucl. Instr. & Methods, **A386** 531 (1997).
- [12] Y. Giomataris *et al.*, Nucl. Instr. & Methods, **A376** 29 (1996).
- [13] The LCTPC Collaboration, <http://www.lctpc.org/>.
- [14] Road map for ILC Detector R&D Test Beams, KEK Report 2007-3, July 2007.
- [15] H. Hillert, in these proceedings.
- [16] V. Morgunov and A. Raspereza, arXiv:physics/0412108.
- [17] T. Yoshioka, ECONF C0508141:ALCPG1711,2005.
- [18] M.A. Thomson, arXiv:physics/060726.
- [19] O. Wendt, in these proceedings.
- [20] D. Barbareschi *et al.*, <http://www.4thconcept.org/DCR.pdf> <http://www.4thconcept.org>
- [21] See <http://physics.uoregon.edu/~lc/historical-examples.html>.